arXiv:1208.4882v1 [cond-mat.supr-con] 24 Aug 2012

Magnetic field-induced parity and time-reversal symmetry broken superconducting state in LiFeAs

G. Li,[1] R. R. Urbano,[1, 2] P. Goswami,[1] C. Tarantini,[1] B. Lv,[3] P. Kuhns,[1] A. P. Reyes,[1] C. W. Chu,[3] and L. Balicas[1, *]

[1] *National High Magnetic Field Laboratory, Florida State University, Tallahassee-FL 32310, USA*
[2] *Instituto de Física "Gleb Wataghin", UNICAMP, 13083-859 Campinas, Brazil*
[3] *Texas Center for Superconductivity, University of Houston, Houston, Texas 77204-5002, USA*

(Dated: August 27, 2012)

Magnetometry measurements in high quality LiFeAs single-crystals reveal a change in the sign of the magnetic irreversibility in the vicinity of the upper critical H_{c2}, i.e. from a clear diamagnetic-like response dominated by the pinning of vortices, to a state with a considerably smaller paramagnetic-like irreversibility which *disappears* at H_{c2}. If diamagnetism results from screening super-currents, paramagnetism must result from currents circulating in the opposite sense, mimicking a field-dependent magnetic moment *below* H_{c2}. We conclude that the superconducting state of LiFeAs at high fields must break time-reversal and parity symmetries. A Ginzburg-Landau analysis indicates that the field could stabilize a gap wave-function with either $(d_{x^2-y^2} + id_{xy})$ or $(p_x + ip_y)$ symmetry, implying that LiFeAs might display a field-induced topological superconducting state.

PACS numbers: 74.70.Xa, 74.25.Dw, 74.62.Dh, 74.25.fc

LiFeAs [1] is a stoichiometric compound belonging to the new family of layered iron pnictides which displays a superconducting transition at a critical temperature $T_c \simeq 18$ K. In contrast to most Fe based superconductors, LiFeAs becomes superconducting without doping a parent metallic antiferromagnet [2]. Local Density Approximation (LDA) calculations indicate that the Fermi surface of virtually all non-magnetic Fe pnictide compounds is composed of two cylindrical sheets of electron character at the M point and, depending on the doping level, of at least two more cylinders of hole-character at the Γ point of the first Brillouin zone (FBZ) [3]. In the simplest scenarios [3], antiferromagnetism is believed to emerge from a Peierls-like instability associated with nearly nested electron- and hole-like cylindrical Fermi-surfaces (FS). Therefore, from the perspective of band structure calculations LiFeAs should display itinerant antiferromagnetism instead of a superconducting ground state [3]. This tendency to antiferromagnetism would produce antiferromagnetic fluctuations claimed to be responsible for the superconducting pairing mechanism [4]. Although, for these multi-orbital systems characterized by strong Hund's coupling, alternative pairing scenarios including triplet pairing, have been proposed [5].

Initial angle resolved photoemission spectroscopy (ARPES) studies indicated very different relative sizes for the electron and hole-like FSs, implying the absence of FS nesting and concomitant itinerant magnetism [6]. This same study, in contrast to Ref. 7 but in agreement with more recent measurements [8], finds that superconductivity in LiFeAs is multi-band in nature with gaps in both sets of FSs. This conclusion is supported by a series of penetration depth studies [9–11] which finds at least two s-wave gaps whose relative amplitudes is within a factor of 2, also with heat-capacity [12] and nuclear magnetic resonance studies which find the relative size between both gaps to be within a factor of approximately three [2, 14]. Multi-band superconductivity would be in agreement with the so-called $s\pm$ state [4] whose corresponding gap wave-function has nodes located in between the cylindrical FSs. The application of high magnetic fields has lead to distinct phase diagrams [3–5] with the values of the superconducting upper-critical fields extrapolated to zero temperature ($H_{c2}(T \rightarrow 0K)$) varying by more than 30 % [3–5]. This suggests that the superconductivity in LiFeAs is particularly sensitive to impurities or variations in stoichiometry. Remarkably, the superconducting phase-boundary at low Ts for in-plane fields was claimed [5] to show evidence for the Fulde-Ferrel-Larkin-Ovchinnikov (FFLO) state [18]. For fields applied along the c-axis thermal conductivity finds no evidence for a field-induced phase-transition [19].

In order to clarify i) the geometry of the FS through the de Haas van Alphen-effect and ii) the potential existence of additional phases within the superconducting phase diagram we performed magnetic torque and magnetization measurements at high fields in high quality single crystals of LiFeAs with a middle point superconducting transition temperature $T_c \simeq 17.1$ K. The quality of our samples is indicated by the observation of the de Haas-van-Alphen-effect and by the ^{75}As NMR spectrum which indicates the absence of magnetism or inhomogeneities. The de Haas van Alphen results indicate that the hole-like cross sectional areas of the FS are probably considerably smaller than the ones predicted by band structure calculations explaining the absence of antiferromagnetism. In particular, we observe a reversal in the sign of the magnetic irreversibility/hysteresis, i.e. from diamagnetic to paramagnetic-like, within the superconducting state of LiFeAs at high fields indicating the presence of time-reversal symmetry breaking super-currents. This points towards the field-induced suppression of the rota-

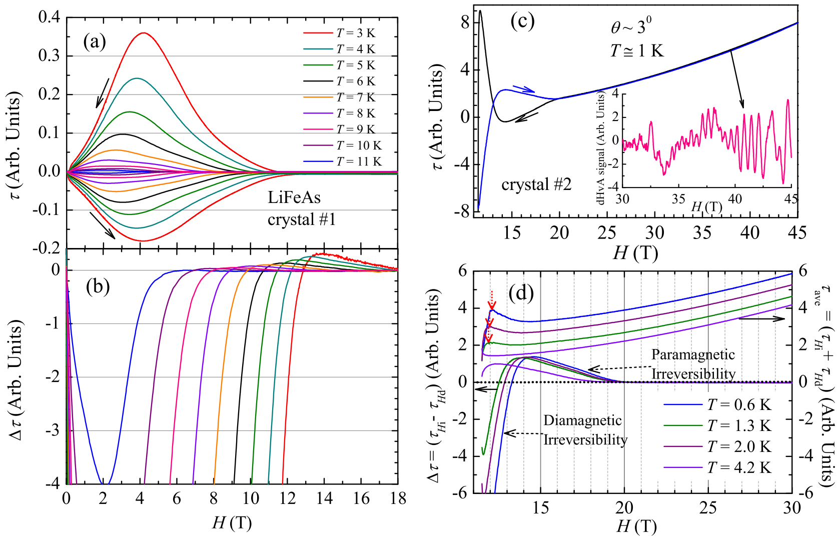

FIG. 1. (color online) (a) Magnetic torque τ as a function of the magnetic field H applied along a direction nearly perpendicular to the inter-layer c-axis of a LiFeAs single crystal (crystal $\sharp 1$) at several temperatures T. This crystal was cleaved from a larger crystal in order to expose fresh and shiny surfaces, and to define a precise rectangular geometry. For each T both the increasing ($H_{\rm inc}$) and decreasing ($H_{\rm dec}$) field sweeps are included. The asymmetry between increasing and decreasing torque branches is due to the extremely large diamagnetic signal which puts our device within the regime of non-linear response. The linear regime and concomitant symmetry is recovered at higher fields (i.e. with the suppression of the diamagnetism). The large hysteretic response in the magnetic torque or the diamagnetic irreversible component, defined as the difference between both branches $\Delta\tau = (H_{\rm inc} - H_{\rm dec})$ *when normalized by the field* is normally proportional to the superconducting critical current (and concomitant pinning forces) according to the Bean model [20]. (b) $\Delta\tau$ (in an amplified scale) as a function of H and for several Ts as extracted from the traces in the top panel. Notice how the diamagnetic signal is followed by an anomalous paramagnetic irreversibility at higher fields which grows as T is lowered. (c) τ as a function of H, for fields between 11.5 to 45 T, at $T = 3$ K and for an angle $\theta = 3^\circ$ between H and inter-planar c-axis, for a second LiFeAs single-crystal. Notice the presence of a second rather symmetric hysteresis loop whose sign is opposite to the diamagnetic one observed at lower fields. Once this second loop closes one observes the expected H^2 dependence for the paramagnetic response: for a layered system one can readily demonstrate that $\tau = \mu_0/2(\chi_{aa} - \chi_{zz})H^2 \sin 2\theta$ where χ_{aa} and χ_{zz} are the in-plane and the out of plane components of the susceptibility tensor, respectively. Once this term is subtracted by fitting it to a quadratic polynomial, an oscillatory component is observed, i.e. the de Haas van Alphen effect (shown in the inset). (d) Respectively, $\Delta\tau$ (left vertical axis) and the average $\tau_{\rm ave}$ between both field-increasing and decreasing torque traces (right vertical axis), for a few temperatures (curves are vertically displaced for clarity). This average is proportional to the reversible quadratic component in the magnet torque except at lower fields where one observes an anomaly (red vertical arrows) which becomes more pronounced as T is lowered. This anomaly is observed well inside the irreversible diamagnetic region suggesting a possible phase transition.

tional symmetry of the original superconducting order-parameter in favor of a multi-component odd parity one, which lacks time-reversal symmetry, and leads to a finite orbital magnetic moment along the external field.

LiFeAs single-crystals were synthesized by using LiAs flux method. Bulk superconductivity was observed in crystals through heat capacity measurements with an onset at ~ 16 K. Torque measurements were performed by using a capacitive cantilever beam configuration. Resistance measurements were performed by using a four terminal configuration. Torquemeters were placed on a single-axis rotator inserted into either a ^{4}He cryostat coupled to a superconducting magnet or a ^{3}He cryostat coupled to the 45 T hybrid-magnet. The angle was measured with Hall probes. Magnetization was measured in a vibrating sample magnetometer, coupled to a superconducting magnet. The same crystals used for the magnetometry measurements were mounted on a NMR probe equipped with a single axis goniometer, which allowed a fine alignment of the crystallographic axis with the external field.

The upper panel of Fig. 1 (a) shows the magnetic torque $\overrightarrow{\tau} = \mu_0 \overrightarrow{M} \times \overrightarrow{H}$, where $\overrightarrow{M}$ is the bulk magnetization, for a LiFeAs single crystal as a function of the field H applied nearly parallel to the inter-layer direction and for several temperatures. One observes a pronounced hysteresis loop $\Delta\tau = (\tau_{H_i} - \tau_{H_d})/2$ between increasing (H_i) and decreasing (H_d) field sweeps (indicated by the arrows), which according to the standard Bean model [20] is proportional to the superconducting critical current J_c, or $\Delta\tau \propto \Delta M \propto J_c = F_p/\mu_0 H$ where F_p is the vortex pinning force density. The vortex pinning mechanisms in LiFeAs have already been studied by other groups [21] and it is not the focus of this manuscript.

Fig. 1 (b) shows a remarkable change in the sign of the magnetic hysteresis/irreversibility, from the diamagnetic- to a paramagnetic-like response. This rather small paramagnetic irreversibility grows as the temperature is lowered and progressively disappears as the field increases in contrast to what is expected for a field-induced magnetic state, indicating that it is intrinsically associated with the superconducting order parameter. We changed the magnet sweep rate from 0.5 to 0.05 T/min, obtaining exactly the same curve(s). This remarkable behavior is more evidently exposed in Fig. 1 (c) which shows τ as a function H and for fields between 11.5 and 45 T at a temperature of 1 K and an angle $\theta = 3^0$ between H and the c-axis of the crystal. At $H \sim 13$ T the diamagnetic hysteresis loop closes and a second loop of opposite sign emerges. When this second loop closes one observes a H^2-dependent behavior as expectable for a paramagnetic state, which can be subtracted revealing an oscillatory component, i.e. the de Haas van Alphen effect (dHvA). A detailed dHvA study in LiFeAs is not among the objectives of this letter nevertheless below we advance a few implications of our observations. Fig. 1 (d) shows both the average τ_{ave} between field-increasing and -decreasing τ branches as well as $\Delta\tau$ for several temperatures. $\Delta\tau$ behaves similarly as in (a), while τ_{ave} which at larger fields (where the irreversibility becomes smaller) is proportional to the reversible or non-hysteretic magnetic response, displays the expected H^2 dependence even within the irreversible region. However, at lower fields a broad anomaly emerges in τ_{ave} sharpening as the temperature is lowered, suggesting a possible phase-transition within the diamagnetic irreversible region.

Since the magnetic torque in layered materials is proportional to the anisotropy of the magnetic susceptibility, the behavior shown above could be attributed to a dramatic reconfiguration of the vortex matter, which might lead to a reversal in the relative size of the terms in the susceptibility tensor thus changing the sign of the torque. To study this possibility we performed magnetization $M = \chi_{zz} H$ measurements in the same single crystals. The results are summarized in figure 2. The important observation is that M, *measured through a quite distinct experimental technique*, also shows an anomalous paramagnetic irreversibility which is at least 1000 times smaller than the corresponding diamagnetic one; *notice how this signal disappears as the field increases* on approaching H_{c2}, indicating that it is *not* associated to localized moments or magnetic domains.

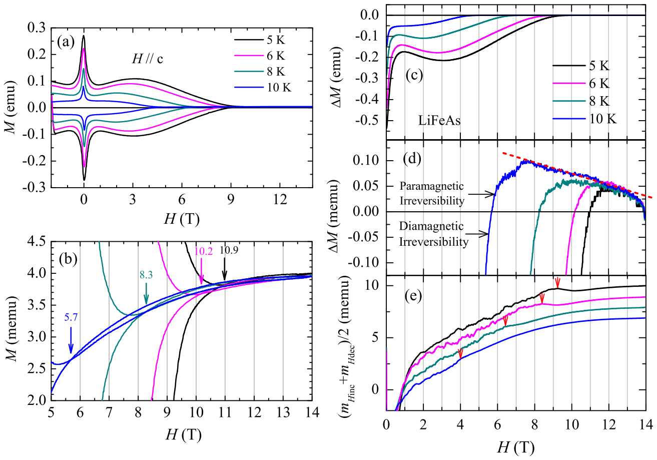

FIG. 2. (color online) (a) Magnetization M as a function of H applied along the inter-planar direction for a few temperatures, and respectively for increasing and decreasing field sweeps. (b) Same as in (a) but in a limited field and magnetization range. This data was acquired by using a vibrating sample magnetometer. Notice that the magnetization $M = \chi_{zz} H$ branches, similarly to the torque data, also cross at higher fields. (c) Pure irreversible component in the magnetization as the difference ΔM between the field increasing and decreasing traces. (d) Same as in (c) but in an amplified scale, showing the crossover from the diamagnetic to a paramagnetic-like irreversibility. Notice that this paramagnetic response is more than 3 orders of magnitude smaller than the diamagnetic one and becomes progressively smaller as the field is increased. (e) Average between both magnetization traces which in the region where the irreversibility becomes smaller is proportional to the reversible component in the magnetization. This so-defined reversible component increases with field and nearly saturates at the highest fields, showing a mild anomaly (red arrows) before saturating.

There are various explanations for a paramagnetic-like Meissner response *at low fields*, also known as the Wohlleben-effect [22–25] which either rely on the small size of the system or in the granularity of the sample. For a weak magnetic field, the magnetic length of the Cooper pair can be comparable to the size of the system for a small superconducting sample. In this case, consideration of surface superconductivity and associated giant vortex state becomes important [22, 23]. The giant vortex state causes flux compression and leads to a paramagnetic Meissner effect in the low field limit. For our experimental set up, at large magnetic fields the magnetic length of the Cooper pair is much smaller than the system size, and quantization of orbital motion is relevant, which leads to the presence of multiple vortices, rather than a giant vortex state. The flux compression can also occur due to surface superconductivity, which is induced by inhomogeneous cooling [24]. For any flux compression picture, the calculated magnetic moment becomes paramagnetic only in the low field limit, and a diamagnetic moment is recovered in the high-field limit. Therefore, a flux compression scenario is not relevant for our experiments. For granular d-wave superconductors one can consider random-junctions [25], which can also cause paramagnetic Meissner effect. However our sample is not granular, and does not demonstrate signatures of d-wave superconductivity at zero or low fields. Therefore, for our experiments the π-junction scenario is also invalid. As discussed in the Supplemental Information linked to this manuscript [29], the observation of the de Haas van Alphen effect, particularly a series of frequencies or Fermi Surface cross-sectional areas, and a single narrow Lorentzian ^{75}As NMR peak are very strong indications for a homogeneous high quality single crystal.

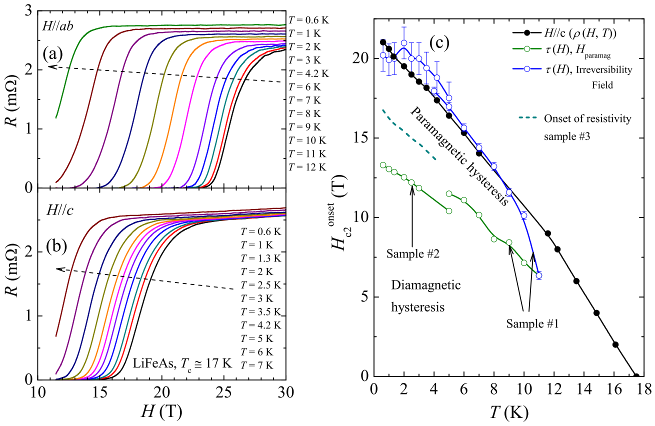

FIG. 3. (color online) (a) Resistance for a LiFeAs single crystal as a function of H applied along a planar direction and for several temperatures. Here, the electrical current flows along a planar direction perpendicular to the external field. (b) Same as in (a) but for fields applied along the inter-planar direction. (c) From the data in Figs. 1, 4(a) and 4(b) superconducting phase diagram for LiFeAs for fields along the inter-planar direction as resulting from the present study: green markers connected by green lines depict the boundary between the diamagnetic and the paramagnetic irreversible behaviors, while the blue lines correspond to the irreversibility field H_{irr} or the onset of the paramagnetic *reversible* behavior. Black markers depict the onset of the superconducting transition for fields along the c-axis, i.e. the point in temperature where the resistance reaches 90 % of its value in the normal state just prior to the transition (sample ♯3). Darker dashed green line depicts the foot of the resistive transition, i.e. the point in temperature where the resistance emerges from its zero value (sample ♯3 in (a)).

Figures 3 (a) and (b) show the resistance R as function of H applied along two orientations, i.e. a planar direction and the inter-planar axis, for a LiFeAs single crystal and for several temperatures, respectively. This data is used to determine $H_{c2}(T)$ as shown in Fig. 4 **c**, which includes data only for fields oriented along the c-axis, although we have also observed the anomalous irreversible response for fields close to the ab-plane. The superconducting region characterized by the paramagnetic irreversibility only emerges below 11 K, occupying a large portion of the phase diagram at lower temperatures and higher fields suggesting that it is not a property of the superconducting state at zero-field. One also observes a remarkable agreement for the high-field phase-boundary between torque and resistivity measurements.

Broken time reversal symmetry within superconductivity was observed in CeCoIn$_5$ at low temperatures and high fields and associated with the coexistence of magnetism with a putative FFLO state [27]. This would be an intriguing possibility for LiFeAs which would agree with the claims of Ref. 5, although the comparatively much larger area occupied by the anomalous state in the diagram of Fig. 3 (c), points towards an alternative scenario. In effect, our experiments can be reconciled with a superconducting state that breaks both parity and time reversal symmetries. Here, we assume that the low field (below H_{c1}) superconducting phase is the fully gapped $s\pm$ state which is stable against other competing pairing channels. Nevertheless, in the mixed state and close to H_{c2}, the Bogoliubov-de Gennes quasiparticles of a generic type II superconductor become gapless at special points in the Brillouin zone associated with the vortex lattice [28]. These gapless quasiparticles can be susceptible to competing pairing channels, which were innocuous for the low field fully gapped state. The effects of competing pairing channels in the mixed phase can also be understood within a phenomenological Landau-Ginzburg theory (see discussion in Supplemental Information [29]). There are gradient couplings among different singlet order-parameters, and the Zeeman splitting allowing a Lifschitz invariant in the free energy functional [30], which couples triplet p-wave order parameters to the gradient of the $s\pm$ order parameter [31]. In the presence of such inter-channel couplings, the super-current of the $s\pm$ state can give rise to a singlet $(d_{x^2-y^2} + id_{xy})$ or a triplet $(p_x + ip_y)$ pairing component in the mixed phase. The induced triplet component is a unitary state with zero spin projection along the magnetic field [31]. The competing chiral components carry finite orbital magnetic moment along the external field, which also leads to a paramagnetic response.

In comparison to the 122 Fe-pnictides, in LiFeAs the nesting between electron- and hole-like Fermi surfaces is far more imperfect [6]. This could increase the strength of the d-wave fluctuations when compared to the $s\pm$ pairing channel. ARPES [6] also suggests the presence of shallow hole-pockets and a van Hove singularity at the zone center, which can cause significant ferromagnetic fluctuations leading to a nonzero coupling constant in the triplet pairing channel. At present it is unclear which of these competing channels is stabilized, but our results open the possibility of a field-induced topological superconducting state with Abelian excitations [32]. Added note: we recently tried to detect the de Haas van Alphen-effect (dHvA) in 4 crystals from the same original batch: although these crystals still display virtually the same T_c and resistivity ratio, we were unable to observe either the dHvA oscillations or the paramagnetic irreversibility, suggesting that extreme sample quality is required for observation of both effects.

The NHMFL is supported by NSF through NSF-DMR-0084173 and the State of Florida. L. B. is supported by

DOE-BES through award de-sc0002613.

---

[*] balicas@magnet.fsu.edu

[1] J. H. Tapp, *et al.*, Phys. Rev. B **78**, 060505 (2008).
[2] R. H. Liu *et al.* , Phys. Rev. Lett. **101**, 087001 (2008).
[3] D. J. Singh, Phys. Rev. B **78**, 094511 (2008).
[4] I. I. Mazin, D. J. Singh, M. D. Johannes, and M. H. Du, Phys. Rev. Lett. **101**, 057003 (2008).
[5] X. Dai, Z. Fang, Y. Zhou, and F. -C. Zhang, Phys. Rev. Lett. **101**, 057008 (2008); P. A. Lee and X. -G. Wen, Phys. Rev. B **78**, 144517 (2008); S. Raghu, X. -L. Qi, C. -X. Liu, D. J. Scalapino, and S. -C. Zhang, Phys. Rev. B **77**, 220503(R) (2008).
[6] S. V. Borisenko *et al.* , Phys. Rev. Lett. **105**, 067002 (2010).
[7] D. S. Inosov *et al.* , Phys. Rev. Lett. **104**, 187001 (2010).
[8] K. Umezawa *et al.* , Phys. Rev. Lett. **108**, 037002 (2012).
[9] Y. J. Song *et al.*, EPL **94**, 5700 (2011).
[10] H. Kim, M. A. Tanatar, Y. J. Song, Y. S. Kwon, and R. Prozorov, Phys. Rev. B **83**, 100502(R) (2011).
[11] K. Hashimoto *et al.* , Phys. Rev. Lett. **108**, 047003 (2012).
[12] F. Wei *et al.* , Phys. Rev. B **81**, 134527 (2010).
[13] Z. Li *et al.* , J. Phys. Soc. Jpn. **79**, 083702 (2010).
[14] P. Jeglic *et al.* , Phys. Rev. B **81**, 140511 (2010).
[15] J. L. Zhang *et al.* , Phys. Rev. B **83**, 174506 (2011).
[16] S. Khim *et al.* , Phys. Rev. B **84**, 104502 (2011).
[17] K. Cho *et al.* , Phys. Rev. B **83**, 060502 (2011).
[18] See, H. Burkhardt, and D. Rainer, Ann. Phys. -Berlin **506**, 181 (1994), and references therein.
[19] M. A. Tanatar *et al.* , Phys. Rev. B **84**, 054507 (2011).
[20] C. P. Bean, Phys. Rev. Lett. **8**, 250 (1962).
[21] A. K. Pramanik *et al.* , Phys. Rev. B **83**, 094502 (2011).
[22] A. K. Geim, S. V. Dubonos, J. G. S. Lok, M. Henini, and J. C. Maan, Nature **396**, 144 (1998).
[23] V. V. Moshchalkov, X. G. Qiu, and V. Bruyndoncx, Phys. Rev. B **55**, 11793 (1997).
[24] A. E. Koshelev and A. I. Larkin, Phys. Rev. B **52**, 13559 (1995) and references therein.
[25] M. Sigrist and T. M. Rice, Rev. Mod. Phys. **67**, 503 (1995) and references therein.
[26] C. Putzke *et al.*, Phys. Rev. Lett. **108**, 047002 (2012).
[27] M. Kenzelmann *et al.* , Science **321**, 1652 (2008).
[28] M. Rasolt and Z. Tesanovic, Rev. Mod. Phys. **64**, 709 (1992).
[29] See Supplemental Material at http://link.aps.org/supplemental.
[30] V. P. Mineev, and K. V. Samokhin, JETP **78**, 401 (1994).
[31] O. Dutta and A. G. Lebed, Phys. Rev. B **78**, 224504 (2008).
[32] N. Read and D. Green, Phys. Rev. B **61**, 10267 (2000).

Supplemental Information

Introduction

In this Supplemental Information file, we provide enough information to indicate the quality of our single-crystals. For instance, in the “Sample Quality” section we show Squid data that clearly indicates the absence of localized moments or long range magnetic order. In addition, we also discuss the de Haas van Alphen and the ^{75}As nuclear magnetic resonance data, which taken together are very strong indications for a relatively long mean free path in a homogeneous sample. But we also indicate that some degradation or aging process seems to occur in this material, leading to the simultaneous disappearance of the Haas van Alphen-effect and the anomalous paramagnetic irreversibility reported in this manuscript.

Our experimental observations can be reconciled with a superconducting state that breaks both parity and time reversal symmetries. In the low field (below H_{c1}), the $s_{\pm}$ state is fully gapped and stable against other competing pairing channels. However in the mixed state and close to H_{c2}, the Bogoliubov-de Gennes quasiparticles of a generic type II superconductor become gapless at special points in the magnetic Brillouin zone [6]. These gapless quasiparticles can be susceptible to competing pairing channels, which were innocuous in low field fully gapped state. The effects of competing pairing channels in the mixed phase can also be understood within a phenomenological Landau-Ginzburg theory (see below). There are gradient couplings among different singlet order parameters, and the Zeeman splitting allows a Lifschiz invariant in the free energy functional, which couples triplet p wave order parameters to the gradient of $s_{\pm}$ order parameter. In the presence of such inter-channel couplings, the supercurrent of $s_{\pm}$ state can give rise to a singlet $d_{x^2-y^2} + id_{xy}$ or a triplet $p_x + ip_y$ pairing component in the mixed phase. The induced triplet component is a unitary state with zero spin projection along the magnetic field. The competing chiral components are particularly strong in the vortex cores, and carry finite orbital magnetic moment along the external field, which also leads to *paramagnetic response*.

In LiFeAs the electron and hole pockets are much less well nested when compared to the 122 pnictides, and this can increase the strength of d-wave fluctuations compared to $s_{\pm}$ pairing channels. ARPES also suggest the presence of shallow hole pockets and a van Hove singularity at the zone center, which can cause significant ferromagnetic fluctuations, which in turn lead to a nonzero coupling constant in the triplet pairing channel. At present it is not clear which of these competing channels is stabilized, and elaborate future experiments will elucidate this issue. LiFeAs apparently is a unique material within the Fe-pnictide family, which has competing pairing channels, and our results indicate that this competition leads to a parity and time-reversal symmetry-breaking chiral pairing component in the high-field mixed state, as described in the section treating the Landau-Ginzburg formalism.

Sample quality

Absence of localized moments

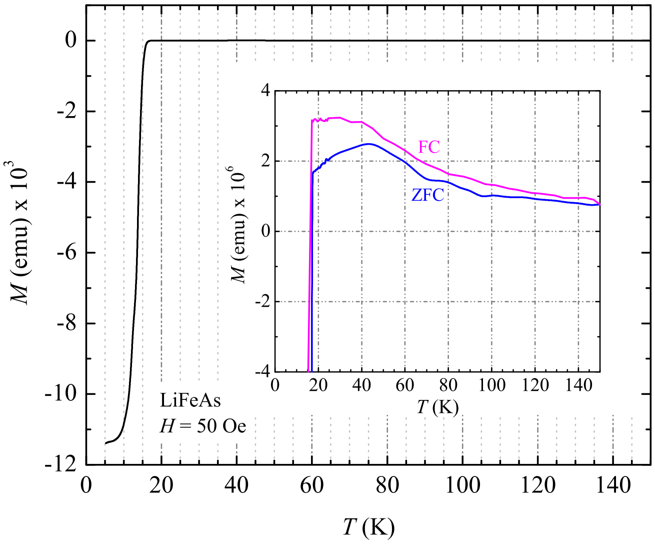

FIG. 4. (color online) Main panel: Magnetization (M) as a function of the temperature for one of our LiFeAs single crystals acquired under a field of 50 Oe and after cooling the sample at zero field. Inset: M as a function of temperature but in an amplified scale showing the magnetic response of the metallic state under zero-field- (blue line) and under field-cooled (magenta line) conditions. The apparent hysteresis is an experimental artifact, since the magnetic response of the metallic state is comparable in magnitude to the sensitivity of the instrument.

The supplementary Fig. 1 below shows the magnetization as a function of the temperature for one of our LiFeAs single crystals. As seen, the magnetic response of the metallic state is several orders of magnitude smaller than the diamagnetic response characteristic of the superconducting phase. This signal is comparable to the level of sensitivity of our commercial Squid magnetometer. This by itself, points towards the absence of localized Fe moments which would provide a very sizeable contribution, i.e. comparable to the diamagnetic one. This is further confirmed by the temperature dependence of the metallic state magnetization, which does not display the characteristic Curie-Weiss susceptibility expectable for localized magnetic moments. To this, one has to add the absence of any evidence suggesting long-range magnetic-order in this system. Therefore, we can very safely discard localized magnetic moments, or conventional magnetism, as a potential source for a paramagnetic like irreversible response in LiFeAs.

High quality single crystals: De Haas van Alphen oscillations and ^{75}As nuclear magnetic resonance measurements

To expose the quality of our crystals, we show in the supplementary Figs. 2 (a), (b), and (c) the oscillatory component superimposed into our torque signal as a function of H^{-1} (de Haas van Alphen signal), a Fast Fourier transform of the oscillatory signal, and the temperature dependence of the ^{75}As NMR spectrum taken in the same single crystals used for torque and magnetization measurements, respectively. The goal of this figure is to demonstrate the extreme high quality of our crystals with no clear evidence for either impurities or magnetism. In effect, under a magnetic field, the crossing of the quantized electronic orbits (Landau levels) through the Fermi level produces oscillatory components in M, i.e. the dHvA-effect, which are periodic in H^{-1} and whose fundamental frequencies

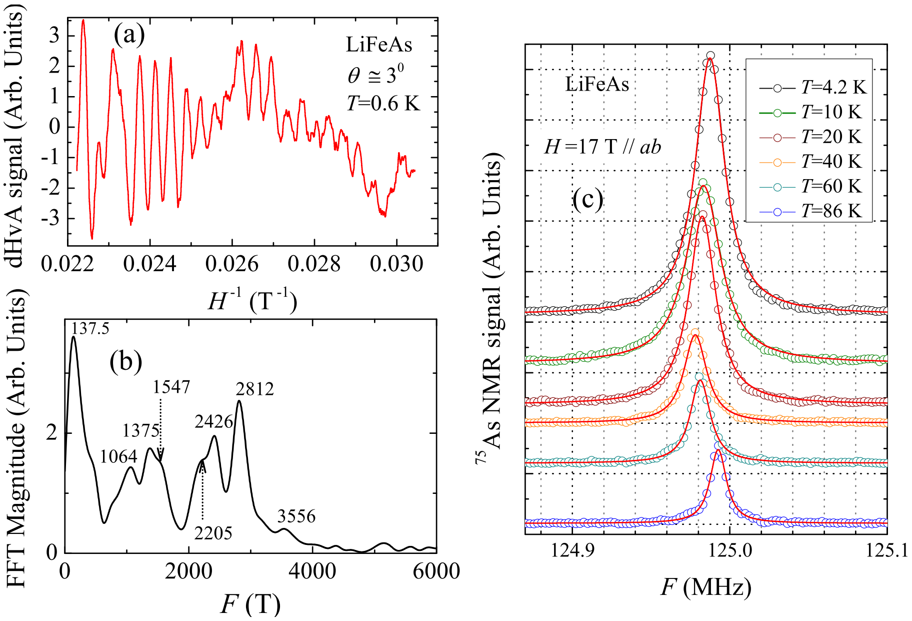

FIG. 5. (color online) (a) Oscillatory component, or the de Haas van Alphen effect superimposed onto the torque signal of a LiFeAs single crystal within its paramagnetic phase as a function of the inverse field H^{-1}, at a temperature $T = 0.6$ K and an angle $\theta = 3^\circ$ between the magnetic field and the inter-planar c-axis. (b) Magnitude of the fast Fourier transform of the oscillatory signal shown in (a) as a function of the cyclotronic frequency, showing at least 5 clear peaks and indications for several additional frequencies. (c) Temperature dependence of the ^{75}As NMR spectra for the same LiFeAs single-crystal with the magnetic field applied along the planar direction ($H \| ab = 17$ T). The red solid lines are fits to a single Lorentzian line. The high quality of the fit and the quite narrow line-width (FWHM   22.64 kHz at 4.2 K) observed for our LiFeAs single crystal discard the presence of either short or long range magnetic order. The observation of dHvA oscillations and of narrow Lorentzian NMR lines confirms the extreme high quality of our crystals and implies the absence of magnetic impurities or extrinsic phases.

F are directly related to the extremal cross-sectional areas A of the FS perpendicular to H through the Onsager relation: $F = A(\hbar/2\pi e)$. To observe dHvA oscillations the system must satisfy $\omega_c \tau \gg 1$, where ω_c is the cyclotron frequency and is the quasiparticle time of flight, i.e. the system must be clean. Band structure calculations predict at least 10 dHvA frequencies for LiFeAs [1]. The fast Fourier transform (FFT) of the dHvA signal yields at least 5 frequencies with indications for at least another 3; in order words we detect more frequencies than those reported in Ref. 1 which were all attributed to cross sections from the electron-like FSs. In addition to observing these, we also detect smaller frequencies, i.e. 138, 1064 and 1375 T, which can only be attributed to hole-like FSs. The last two frequencies are at odds with the calculations shown in Ref. 1, suggesting that the hole-like FSs are actually smaller than the predicted ones, explaining the absence of itinerant magnetism. The observation of a large portion of the FS of LiFeAs, is a very strong indication for the high quality of our single crystals. In Fig. 3 (c) we present the temperature dependence of the ^{75}As NMR spectra with the magnetic field applied along the planar direction ($H \parallel ab = 17$ T). The observed results give further support to our conclusion. The ^{75}As NMR spectra taken at very high fields, which are similar to those shown in Ref. 2, can be fitted to a single Lorentzian line shape, indicating that our sample is rather homogeneous and shows no traces of magnetic instabilities, crystallographic defects, distortions or strain. Within a local (microscopic) point of view, one of the most efficient ways to investigate the origin of electronic and magnetic states is through the analysis of the hyperfine interactions probed in a NMR experiment. At this point it is important to mention that we found the paramagnetic irreversibility to disappear as a function of time, after the Apiezon grease covered single-crystals were briefly exposed to air which is known to degrade their quality, therefore indicating that this behavior is extremely sensitive to sample degradation. In fact, the suppression of this state might explain the differences among the superconducting diagrams in Refs. 3–5.

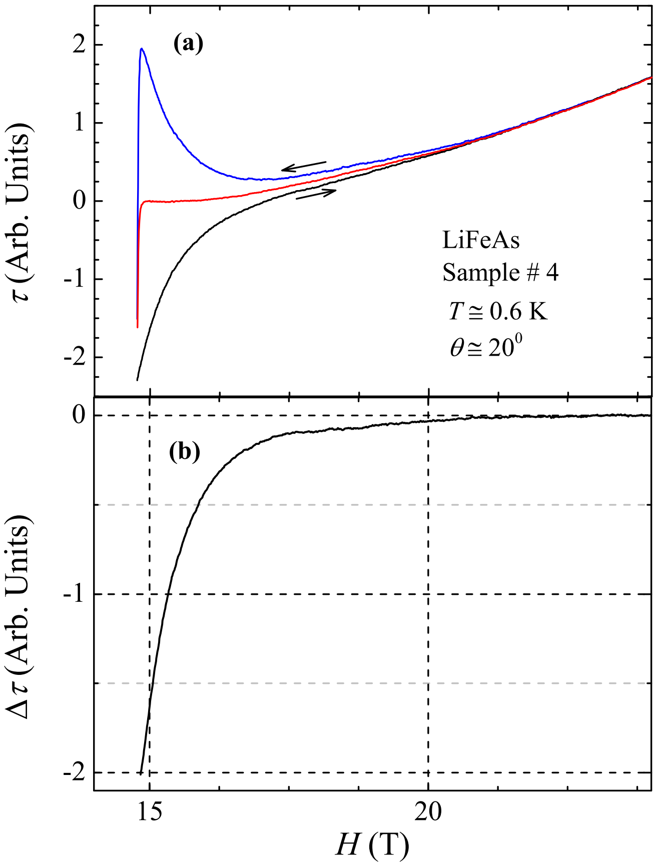

FIG. 6. (color online) (a) Raw magnetic torque as a function of the magnetic field H at temperature $T \simeq 0.6$ K and an angle $\theta \simeq 20^\circ$ between H and the c-axis of the crystal for a fourth LiFeAs single crystal. H is swept between a narrow range of 15 to 23 T, or around the superconducting to metallic phase-transition. Field up and down sweeps are depicted by the black and blue traces, respectively. Red line corresponds to the average between both traces. This single-crystal belongs to the same batch as the previously measured crystals, but does not reveal the anomalous irreversibility nor quantum oscillatory phenomena. It was cleaved from a larger single-crystal in order to reveal fresh shiny surfaces. Its geometry $1.2 \times 1 \times 0.1$ mm^3 is roughly similar to the geometry of crystal ♯1. This observation suggests that the anomalous irreversibility is intrinsically associated with quality of the *bulk* of the single crystal.

Sample quality dependence

In the supplementary Fig. 3 below, we show the magnetic torque for a fourth LiFeAs single crystal in provenance from the same batch as the one used for all three crystals whose measurements are shown above. This measurement was performed nearly one year later with respect to the previous ones. As can be seen in Fig. 1, by using the exact same experimental set-up previously used to uncover the anomalous irreversibility illustrated above, for this specific single crystal the anomalous irreversibility is not observed. We were also unable to observe the de Haas van Alphen effect. Three additional single-crystals of this one year older batch were tested and none revealed either the paramagnetic irreversibility or the de Haas van Alphen effect, indicating a correlation between both effects and between these and the quality of the sample.

This observation or the lack of thereof has several implications: i) The most obvious one is that the anomalous irreversibility cannot be simply attributed to an experimental artefact (although the observation of such irreversibility through a second, quite distinct experimental technique such as vibrating sample magnetometry is already a strong argument in this direction). ii) The similar geometries between crystals ♯1 and ♯4 (both crystals were cleaved with a razor blade in Ar atmosphere in order to display a typical geometry of $1.2 \times 1 \times 0.1$ mm^3 and shiny surfaces) leads one to conclude that the interplay between surface and bulk superconductivities, which was found to lead to an anomalous paramagnetic-like Meissner response in mesoscopic superconductors [14], is not relevant to the present case. Crystal ♯2 which also displayed this anomalous paramagnetic irreversibility was not cleaved, further indicating that the role of the surface is unimportant for this effect. Remarkably, and perhaps unsurprisingly, crystals ♯1 and ♯4, displayed virtually the same T_c (~ 17.1 K and resistivity ratios $R(300K)/R(20K) \geq 20$)

Landau-Ginzburg formalism

Induction of $d + id$ component

We first consider the couplings among A_{1g} $s_{\pm}$, B_{1g} $d_{x^2-y^2}$ and B_{2g} d_{xy} pairing channels. The quadratic part of the free energy functional can be written as $f_{quad} = f_s + f_{x^2-y^2} + f_{xy} + f_{s,x^2-y^2} + f_{s,xy} + f_{x^2-y^2,xy}$, where

$$\begin{aligned} f_s &= K_s(D_j\psi_s)^* D_j\psi_s + r_s|\psi_s|^2 && (1)\\ f_{x^2-y^2} &= K_{x^2-y^2}(D_j\psi_{x^2-y^2})^* D_j\psi_{x^2-y^2} + r_{x^2-y^2}|\psi_{x^2-y^2}|^2 && (2)\\ f_{xy} &= K_{xy}(D_j\psi_{xy})^* D_j\psi_{xy} + r_{xy}|\psi_{xy}|^2 && (3)\\ f_{s,x^2-y^2} &= K_{s,x^2-y^2}[(D_x\psi_s)^* D_x\psi_{x^2-y^2} - (D_y\psi_s)^* D_y\psi_{x^2-y^2} + c.c.] && (4)\\ f_{s,xy} &= K_{s,xy}[(D_x\psi_s)^* D_y\psi_{xy} + (D_y\psi_s)^* D_x\psi_{xy} + c.c.] && (5)\\ f_{x^2-y^2,xy} &= iK_{x^2-y^2,xy}H[\psi^*_{x^2-y^2}\psi_{xy} - \psi^*_{xy}\psi_{x^2-y^2}] && (6) \end{aligned}$$

In the above equations ψ's correspond to the order parameters in different channels, $D_j = \partial_j - i2eA_j$'s are the covariant derivatives and A_j's are the vector potentials in x and y directions. H is the external magnetic field. In addition K's and r's are phenomenological coupling constants. The coupling constants can be chosen in a way to produce $s_{\pm}$ state as the ground state for $H < H_{c1}$. For example, we can assume that only r_s changes sign from being positive to negative, as the temperature is lowered below the transition temperature T_c, and $r_{x^2-y^2}$, r_{xy} remain positive in the entire temperature range.

The $f_{x^2-y^2,xy}$ term has been considered in the context of high-T_c cuprate superconductors, to obtain a field-induced id_{xy} component in $d_{x^2-y^2}$ wave superconductors [6]. This term describes the Zeeman coupling of the external field and the orbital angular momentum of $(d + id)$ superconductor. Such a coupling is always allowed by the symmetry, but the size of this coupling can be very small. For our problem of $s\pm$ superconductor, the primary reason for a field-induced $(d + id)$ component are the combined effects of $s - d$ couplings K_{s,x^2-y^2} , $K_{s,xy}$ and the Landau level structure of the $s\pm$ order-parameter. The presence of $f_{x^2-y^2,xy}$ term only enhances the size of the induced $(d + id)$ component.

Immediately below H_{c2}, we can obtain a qualitative understanding of the emergent state by analyzing f_{quad}. In the vicinity of H_{c2}, the solutions are found from the following Landau-Ginzburg equations

$$\begin{aligned} [K_s(D_x^2 + D_y^2) + r_s]\psi_s &\approx 0 && (7)\\ K_{s,x^2-y^2}(D_x^2 - D_y^2)\psi_s + r_{x^2-y^2}\psi_{x^2-y^2} + iK_{x^2-y^2,xy}\psi_{xy} &\approx 0 && (8)\\ K_{s,xy}D_xD_y\psi_s + r_{xy}\psi_{xy} - iK_{x^2-y^2,xy}\psi_{x^2-y^2} &\approx 0 && (9) \end{aligned}$$

The s-wave order parameter ψ_s is described by the lowest Landau level wave function and in the symmetric gauge $\mathbf{A} = (-Hy/2, Hx/2)$ has the spatial dependence $\psi_s \sim \exp[-(x^2 + y^2)/2l^2]$, where l is the magnetic length. The solution for d-wave components are described by

$$\psi_{x^2-y^2} = \frac{[-r_{xy}K_{s,x^2-y^2}(D_{x^2} - D_{y^2}) + iK_{x^2-y^2,xy}HK_{s,xy}D_xD_y]\psi_s}{r_{x^2-y^2}r_{xy} - K^2_{x^2-y^2,xy}h^2} \tag{10}$$

$$\psi_{xy} = \frac{[-r_{x^2-y^2}K_{s,xy}D_xD_y + iK_{x^2-y^2,xy}HK_{s,x^2-y^2}(D_x^2 - D_y^2)]\psi_s}{r_{x^2-y^2}r_{xy} - K^2_{x^2-y^2,xy}H^2} \tag{11}$$

By using the solution for ψ_s, we find $\psi_{x^2-y^2}$ and ψ_{xy} to be respectively real and pure imaginary. Therefore the two d-wave components have a relative phase $\pi/2$, and the mixed state acquires a parity and time reversal symmetry breaking $(d+id)$ component, and carries a finite orbital magnetic moment pointing along the external magnetic field. It also becomes clear from the expressions for d-wave components, that the Zeeman coupling of the $(d + id)$ orbital moment plays a secondary role, and causes enhancement of the d-wave components. We can also take a Abrikosov vortex lattice solution or a trial disordered vortex lattice solution for ψ_s, and still find a corresponding solution for $d + id$ component. According to the above arguments, a $(d + id)$ component can be induced in the mixed state, irrespective of the signs or strengths of $r_{x^2-y^2}$, r_{xy}. However, this component will have observable effects, only if $s - d$ mixing terms are sizable, and r_s becomes comparable to $r_{x^2-y^2}$, r_{xy}. In LiFeAs there is a lack of nesting among electron and hole pockets, and this may reduce the strength of $s_{\pm}$ coupling, and make the d-wave effects relatively stronger.

Singlet-triplet mixing and induction of $p + ip$ component

There can be mixing between singlet and triplet p-wave pairing channels due to Zeeman splitting of fermi surfaces, due to a Lifschiz invariant [8–12] (we do not consider the mixing due to spin-orbit coupling). We can describe the **d** vector of the p-wave pairing as $d_\mu = d_{\mu j}\hat{x}_\mu p_j$, where $\hat{x}$ is a unit vector in the spin space and couples to the Pauli matrices, p_j is the components of relative momentum. We can write the quadratic part of the free energy as $f_{quad} = f_s + f_p + f_{s,p}$, where

$$\begin{aligned} f_p &= K_{p1}(D_j d_{\mu a})^*)(D_j d_{\mu a}) + K_{p2}(D_b d_{\mu j})^*)(D_j d_{\mu b}) + K_{p3}(D_b d_{\mu b})^*)(D_j d_{\mu j}) + r_p d^*_{\mu j} d_{\mu j} \\ &\quad - i g_1 \epsilon_{\alpha\mu\nu} H_\alpha d^*_{\mu j} d_{\nu j} + g_2 H_\mu H_\nu d^*_{\mu j} d_{\nu j} \qquad (12) \\ f_{s,p} &= -i g_3 H_\mu d^*_{\mu j} D_j \psi_s + c.c \qquad (13) \end{aligned}$$

where K's, r_p, g_1, g_2 and g_3 are phenomenological coupling constants. The $f_{s,p}$ term is the Zeeman splitting induced Lifshitz coupling among p-wave and s-wave pairing order parameters, and g_1 term describes the coupling between the spin moment of the Cooper pair and the external field. In the context of A-phase of ^3He in the external field [13], and also in certain ferromagnetic triplet superconductors, g_1 term leads to a non-unitary p-wave pairing. If we consider s-wave to be the dominant pairing in the low field limit, we can solve for the following approximate Landau-Ginzburg equations in the vicinity of H_{c2},

$$[K_s(D_x^2 + D_y^2) + r_s]\psi_s \approx 0 \qquad (14)$$

$$-i g_3 H_\mu D_j \psi_s + r_p d_{\mu j} - i g_1 \epsilon_{\mu\alpha\beta} H_\alpha d_{\beta j} + g_2 H_\mu H_\nu d_{\nu j} = 0 \qquad (15)$$

If we choose the field along z direction, and $\psi \sim \exp[-(x^2 + y^2)/2l^2]$, only nonzero p-wave components are d_{3j}, and

$$d_{3j} = \frac{i g_3 H D_j \psi_s}{r_p + g_2 H^2} \qquad (16)$$

and leads to a unitary, $S_z = 0$, chiral $(p_x + ip_y)$ pairing. In the tilted field, the equations become more cumbersome, but we always find a chiral $S_z = 0$ paired state. The effects of such chiral p-wave component can be observable only for a sizable $g_3 H$ and comparable s-wave and p-wave couplings. In general disorder induced broadening effects can diminish the inter-channel couplings, and therefore the emergent chiral state will be fragile against disorder effects.

---

[*] balicas@magnet.fsu.edu

[1] C. Putzke *et al.*, Phys. Rev. Lett. **108**, 047002 (2012).
[2] Z. Li *et al.* , J. Phys. Soc. Jpn. **79**, 083702 (2010).
[3] J. L. Zhang *et al.* , Phys. Rev. B **83**, 174506 (2011).
[4] S. Khim *et al.* , Phys. Rev. B **84**, 104502 (2011).
[5] K. Cho *et al.* , Phys. Rev. B **83**, 060502 (2011).
[6] M. Rasolt, and Z. Tesanovic, Rev. Mod. Phys. **64**, 709 (1992).
[7] A. V. Balatsky, Phys. Rev. B **61**, 6940 (2000).
[8] V. P. Mineev and K. V. Samokhin, JETP **78**, 401 (1994).
[9] K. V. Samokhin and M. S. Mar'enko, Phys. Rev. Lett. **97**, 197003 (2006).
[10] V. V. Kabanov, Phys. Rev. B **76**, 172501 (2007).
[11] O. Dutta and A. G. Lebed, Phys. Rev. B 78, 224504 (2008).
[12] Z. Zheng, and D. F. Agterberg, Phys. Rev. B **82**, 024506 (2010).
[13] D. Vollhardt and P. Wölfle, *The Superfluid Phases of Helium 3* (Taylor & Francis, London, 1990).
[14] A. K. Geim, S. V. Dubonos, J. G. S. Lok, M. Henini, and J. C. Maan, Nature **396**, 144 (1998).